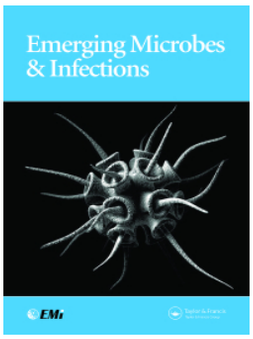

Emerging Microbes & Infections

ISSN: (Print) (Online) Journal homepage: www.tandfonline.com/journals/temi20

Enhanced variant neutralisation through glycan masking of SARS-CoV-2 XBB1.5 RBD

Joey Olivier, Charlotte George, Chloe Qingzhou Huang, Sneha B. Sujit, Paul Tonks, Diego Cantoni, Joe Grove, Laura O'Reilly, Johannes Geiger, Christian Dohmen, Verena Mummert, Anne Rosalind Samuel, Christian Plank, Rebecca Kinsley, Nigel Temperton, Martina Pfranger, Ralf Wagner, Jonathan L Heeney, Sneha Vishwanath & George W. Carnell

To cite this article: Joey Olivier, Charlotte George, Chloe Qingzhou Huang, Sneha B. Sujit, Paul Tonks, Diego Cantoni, Joe Grove, Laura O'Reilly, Johannes Geiger, Christian Dohmen, Verena Mummert, Anne Rosalind Samuel, Christian Plank, Rebecca Kinsley, Nigel Temperton, Martina Pfranger, Ralf Wagner, Jonathan L Heeney, Sneha Vishwanath & George W. Carnell (06 May 2025): Enhanced variant neutralisation through glycan masking of SARS-CoV-2 XBB1.5 RBD, Emerging Microbes & Infections, DOI: 10.1080/22221751.2025.2502011

To link to this article: https://doi.org/10.1080/22221751.2025.2502011

Publisher: Taylor & Francis & The Author(s). Published by Informa UK Limited, trading as Taylor & Francis Group, on behalf of Shanghai Shangyixun Cultural Communication Co., Ltd
Journal: *Emerging Microbes & Infections*
DOI: 10.1080/22221751.2025.2502011

Enhanced variant neutralisation through glycan masking of SARS-CoV-2 XBB1.5 RBD

Authors

Joey Olivier[1], Charlotte George[1], Chloe Qingzhou Huang[1], Sneha B. Sujit[2], Paul Tonks[1], Diego Cantoni[3], Joe Grove[3], Laura O'Reilly[1], Johannes Geiger[5], Christian Dohmen[5], Verena Mummert[5], Anne Rosalind Samuel[5], Christian Plank[5], Rebecca Kinsley[2], Nigel Temperton[4], Martina Pfranger[6,7], Ralf Wagner[2,6,7], Jonathan L Heeney[1,2], Sneha Vishwanath[1,2*], George W. Carnell[1,2,8*].

* Authors contributed equally

1. Lab of Viral Zoonotics, Department of Veterinary Medicine, University of Cambridge, Cambridge, UK

2. DIOSynVax Ltd, University of Cambridge, Cambridge, UK

3. MRC-University of Glasgow Centre for Virus Research, University of Glasgow, Scotland, UK

4. Viral Pseudotype Unit, Medway School of Pharmacy, The Universities of Kent and Greenwich at Medway, Chatham, UK

5. Ethris GmbH, Planegg, Germany

6. Institute of Medical Microbiology and Hygiene, University of Regensburg, Regensburg, Germany

7. Institute of Clinical Microbiology and Hygiene, University Hospital Regensburg, Regensburg, Germany

8. One Virology, Wolfson Centre for Global Virus Research, School of Veterinary Medicine and Science, University of Nottingham, United Kingdom

1. Main Text

Since its emergence in August 2022, the XBB lineage of SARS-CoV-2 has driven multiple waves of SARS-CoV-2 infection worldwide. It has given rise to Variants of Interest (VOIs; XBB.1.5, XBB.1.16, and EG.5) and in July 2023, a new Omicron subvariant emerged – BA.2.86, which gave rise to the lineage JN.1[1,2]. Despite carrying more than 30 mutations in its spike protein relative to its BA.2 variant, BA.2.86 was shown not to be more immune evasive than other circulating variants[1,2]. However, the danger posed by BA.2.86 lies in its distinct antigenicity, improved ACE2 binding affinity and high transmission worldwide which resulted in the emergence of JN.1[3]. This allowed BA.2.86 to persist through population transmission and afforded it the opportunity to evolve a more immune evasive variant, JN.1. JN.1 carries a L455S mutation in its spike that is not present in BA.2.86[4]. In December 2023, the WHO recommended XBB.1.5 as the antigen in monovalent mRNA vaccines as it was demonstrated that the vaccine induced broadly neutralizing and cellular immune responses against EG.5.1 and emerging XBB variants. In our study, we employed glycan masking to the receptor binding domain (RBD) of the SARS CoV-2 XBB.1.5 spike protein using mRNA-LNPs as delivery modality. By introducing the P521N modification to mask the site of CR3022 binding, a neutralising epitope for SARS-CoV, but not for SARS-CoV-2, we aimed to enhance elicitation of neutralising antibodies to SARS-CoV-2 variants by diverting the immune response to neutralising epitopes.

We have previously used the immune focusing approach of epitope masking in a proof-of-concept study in mice demonstrating that glycan modified RBD vaccines (delivered as DNA-prime MVA-boost regimen) generate potent binding and neutralising antibody responses to the different SARS-CoV-2 lineages tested[5]. Here, we employ the same approach to an updated SARS-CoV-2 XBB.1.5 RBD and leverage the strengths of the mRNA platform developed by Ethris GmbH (http://www.ethris.com) in outbred guinea pigs to confirm enhanced immunogenicity of the glycan masked XBB.1.5 RBD vaccine (Fig 1A, Fig 1B, 1C, Supplementary table 1, Supplementary Fig 1-3). We show once again that enhanced neutralising antibody responses are generated when compared to the wild-type control across a panel of lentiviral pseudotypes bearing the native SARS-CoV-2 spike protein from its introduction into humans, subsequent variants and to the currently circulating lineage JN.1.1.

We immunised adult female Hartley guinea pigs twice with 15µg LNP encapsulated mRNA encoding either the membrane tethered RBD of XBB.1.5 (hereby termed XBB.1.5_TM_RBD), the glycan masked RBD of XBB.1.5 (XBB.1.5_TM_M7_RBD), or vehicle controls, with a three-week interval. Blood serum was taken three weeks after prime and three weeks after boost, and terminal sera described here were collected six weeks after the second dose (Fig 1A). Sera were tested for neutralising activity using lentiviral pseudotypes bearing the spike protein from a panel of SARS-CoV-2 variants of concern in pseudotype microneutralisation assays (pMN), which have been shown to correlate with live virus assays[6]. The lentiviral pseudoviruses tested include Wu-Hu-1, Alpha, Beta, Gamma, Delta, BA.1, BA.2, BA.2.75, BA.2.75.2, BA.2.86, JN.1, XBB.1.5, XBB.1.9.1, XBB.1.19.1, BF.7, CH.1.1.1, XBC.1, BQ.1.1, BQ.1.12[7].

When comparing XBB.1.5_TM_M7_RBD to XBB.1.5_TM_RBD, we detected a significant increase in neutralising antibody titre ($Log_{10}IC_{50}$) in terminal sera against the grouped

pseudotyped viruses for XBB.1.5_TM_M7_RBD ($p < 0.0001$, Mann-Whitney U test). Both XBB.1.5_TM_RBD and XBB.1.5_TM_M7_RBD produce a statistically significant difference in neutralising antibody titre compared to the control group ($p < 0.00001$, Mann-Whitney U test). Interestingly, XBB.1.5_TM_M7_RBD elicited increased neutralisation of immune evasive SARS-CoV-2 variants such as BA.2, BA.2.75, BA.2.75.2, BF.7, BQ.1.1, XBB.1.5, XBB.1.9.1, XBB.1.19.1, XBC.1, and JN.1 ($p < 0.05$; Mann-Whitney U-test) (Fig 1D). The largest fold change is seen with JN.1 (6.4) and BA.2 (5.7) (Supplementary Figure 4).

To ascertain whether XBB.1.5_TM_M7_RBD increased neutralisation across the diversity of spike proteins captured in our pseudotype virus panel, we plotted neutralising antibody titres against percentage amino acid identity relative to the Wu-Hu-1 RBD (Fig 1E). Following pairwise comparisons between XBB.1.5_TM_RBD, XBB.1.5_TM_M7_RBD and variant spike RBDs, we found that despite having only one amino acid difference from each other, XBB.1.5_TM_M7_RBD showed increased neutralising antibody titre when compared with XBB.1.5. The neutralising antibody titres for XBB.1.5_TM_M7_RBD are noticeably higher when the amino acid identity is lower when compared to XBB.1.5_TM_RBD, with ellipses in Fig 1E for both constructs indicating the 95% confidence level. The most parsimonious regression tree shows the effect of percentage amino acid identity and construct choice on neutralising antibody titre (Fig 1F) . When factoring in the percentage amino acid identity of the spike protein RBDs neutralised by the antisera, XBB.1.5_TM_M7_RBD elicited higher neutralising antibody titres compared to the native XBB.1.5_TM_RBD sequence. Against spike protein RBDs where the amino acid identity to the vaccine is less than 92%, XBB.1.5_TM_M7_RBD elicited neutralising antibody titres of ±1.5 compared to XBB.1.5_TM_RBD at ±0.71. In the case of a variant having an amino acid identity of more than or equal to 92%, XBB.1.5_TM_M7_RBD (±4.00) also outperformed XBB.1.5_TM_RBD (±3.00) (Fig 1F).

In summary, these results demonstrate significantly greater neutralising antibody titre for XBB.1.5_TM_M7_RBD over the wild type XBB.1.5_TM_RBD, even with adjustment for amino acid similarity. Notably, this improvement in immunogenicity of XBB.1.5_TM_M7_RBD spanned four years of SARS-CoV-2 evolution, from Wu-Hu-1 to the recent JN.1 variant. This work provides further evidence for the strategy of immune focusing by masking a non-neutralising epitope on the SARS-CoV-2 RBD.

2. Discussion

Consistent with our first study, we demonstrate with a recent example that a glycan masking increases the neutralisation capacity of SARS-CoV-2 RBD vaccine antigens. By introducing a single glycosylation site to mask the epitope associated with a binding but non-neutralising antibody (CR3022) on the RBD of SARS-CoV-2 XBB.1.5, we have elicited enhanced neutralising antibodies over that of the wild type antigen. This shows that glycan masking could be a powerful modification in antigen design, potentially future proofing against newly evolving SARS-CoV-2 variants.

When comparing the wild-type vaccine antigen (XBB.1.5_TM_RBD) against the modified vaccine antigen (XBB.1.5_TM_M7_RBD), XBB.1.5_TM_M7_RBD significantly enhanced

neutralisation capacity compared to the wild-type XBB.1.5 variant. This continued into the XBB-lineage, with both XBB.1.9.1 and XBB.1.19.1 spikes also being better neutralised by XBB.1.5_TM_M7_RBD.

JN.1 has less than 97% identity to XBB.1.5_TM_RBD and XBB.1.5_TM_M7_RBD, yet the XBB.1.5_TM_M7_RBD antigen still outperforms XBB.1.5_TM_RBD in terms of neutralisation efficacy. These results are promising considering that a study has shown that JN.1 is more resistant to neutralisation by both XBB.1.5 breakthrough infection and vaccine sera than BA.2.86[4]. This may explain our results where BA.2.86 is neutralised by antisera generated by both XBB.1.5_TM_RBD and XBB.1.5_TM_M7_RBD vaccines with negligible differences, but that XBB.1.5_TM_M7_RBD neutralises JN.1 significantly better than XBB.1.5_TM_RBD.

Antigenic cartography has shown that Omicron variants are antigenically distinct from the earlier VOCs[8]. Within the Omicron lineage, BQ.1 and XBB are not only antigenically distinct from each other, they are also antigenically distinct from early Omicron variants[8]. More recent antigenic maps have shown that BA.2.86 is distinct from D614G, BA.2, BA.5 and XBB.1.5, which suggested potential evasion of XBB-derived neutralising antibodies[9]. BA.2.86's descendant, JN.1, is antigenically distinct and distant from preceding variants[10]. It would be interesting to determine where XBB.1.5_TM_M7_RBD is positioned on these antigenic maps, and more importantly whether it can bridge the antigenic distance between relevant variants.

Hu *et al.* postulated that SARS-CoV-2 has evolved to have five serotypes (Ia, Ib, II – V) based on RBD antigenicity[11]. XBB.1.5_TM_M7_RBD significantly improves neutralisation of pseudotyped viruses that fall in serotypes III (BA.2, BA.2.75), IV (BF.7, BQ.1.1), and V (XBB.1.5). It is likely that BA.2.86 and JN.1 would fall in a separate serotype (putative serotype VI). The BA.2 lineage (serotype III in Hu et al[11]), gave rise to second-generation subvariants that are immune evasive and have driven multiple waves[12]. For example, not only did BA.2.75 exhibit increased immune evasion from vaccinated sera[13] it is also responsible for giving rise to extreme immune evasive variants such as CH.1.1 and XBB[14]. More specifically, XBB is a recombination of two BA.2 lineages, BJ.1 and BM.1.1.1 (derived from BA.2.75)[15]. It is thus reassuring to see that XBB.1.5_TM_M7_RBD significantly increases the neutralisation of BA.2 and its descendants.

In conclusion, our results support antigenically enhanced constructs created by the addition of a glycan mask to improve and broaden their neutralisation capacity. This strategy could serve as a valuable approach to update vaccine antigens, increasing the longevity of vaccine induced antibody responses and making them more resilient against emerging variants.

Acknowledgements:

The authors would like to thank Professor Kei Sato (University of Tokyo) for providing the JN.1 spike expression plasmid. JO, CG, LO, RK, JLH, SV, GWC were funded by CEPI to develop broadly protective coronavirus vaccines. DC and JG[3] were funded by UKRI/MRC code number MC_UU_00034/1. RW and MP were co-funded by the Bavarian States Ministry of Science and Arts (Grant FOR-COVID II to R.W.).

Declaration of interest statement:

SB, RK, RW, JLH, SV and GWC are employees or affiliated to DIOSynVax Ltd, Cambridge, United Kingdom. JG[5], CD, VM, ARS, CP are employees of Ethris GmbH, Munich, Germany. The remaining authors declare no conflicts of interest.

References

1. Khan, K. *et al.* Evolution and neutralization escape of the SARS-CoV-2 BA.2.86 subvariant. *Nat. Commun.* **14**, 8078 (2023).

2. Yang, S. *et al.* Fast evolution of SARS-CoV-2 BA.2.86 to JN.1 under heavy immune pressure. *Lancet Infect. Dis.* **24**, e70–e72 (2024).

3. Wang, Q. *et al.* Antigenicity and receptor affinity of SARS-CoV-2 BA.2.86 spike. *Nature* **624**, 639–644 (2023).

4. Kaku, Y. *et al.* Virological characteristics of the SARS-CoV-2 JN.1 variant. *Lancet Infect. Dis.* **24**, e82 (2024).

5. Carnell, G. W. *et al.* Glycan masking of a non-neutralising epitope enhances neutralising antibodies targeting the RBD of SARS-CoV-2 and its variants. *Front. Immunol.* **14**, 1118523 (2023).

6. Cantoni, D. *et al.* Correlation between pseudotyped virus and authentic virus neutralisation assays, a systematic review and meta-analysis of the literature. *Front. Immunol.* **14**, (2023).

7. Genova, C. *et al.* Production, Titration, Neutralisation, Storage and Lyophilisation of Severe Acute Respiratory Syndrome Coronavirus 2 (SARS-CoV-2) Lentiviral Pseudotypes. *BIO-Protoc.* **11**, (2021).

8. Mykytyn, A. Z., Fouchier, R. A. & Haagmans, B. L. Antigenic evolution of SARS coronavirus 2. *Curr. Opin. Virol.* **62**, 101349 (2023).

9. Yang, S. *et al.* Antigenicity and infectivity characterisation of SARS-CoV-2 BA.2.86. *Lancet Infect. Dis.* **23**, e457–e459 (2023).

10. Wang, Q. *et al.* XBB.1.5 monovalent mRNA vaccine booster elicits robust neutralizing antibodies against XBB subvariants and JN.1. *Cell Host Microbe* **32**, 315-321.e3 (2024).

11. Hu, S. *et al.* Classification of five SARS-CoV-2 serotypes based on RBD antigenicities. *Sci. Bull.* **68**, 3003–3012 (2023).

12. Roemer, C. *et al.* SARS-CoV-2 evolution in the Omicron era. *Nat. Microbiol.* **8**, 1952–1959 (2023).

13. Kurhade, C. *et al.* Low neutralization of SARS-CoV-2 Omicron BA.2.75.2, BQ.1.1 and XBB.1 by parental mRNA vaccine or a BA.5 bivalent booster. *Nat. Med.* **29**, 344–347 (2023).

14. Qu, P. *et al.* Enhanced evasion of neutralizing antibody response by Omicron XBB.1.5, CH.1.1, and CA.3.1 variants. *Cell Rep.* **42**, 112443 (2023).

15. Tamura, T. *et al.* Virological characteristics of the SARS-CoV-2 XBB variant derived from recombination of two Omicron subvariants. *Nat. Commun.* **14**, 2800 (2023).

Figures

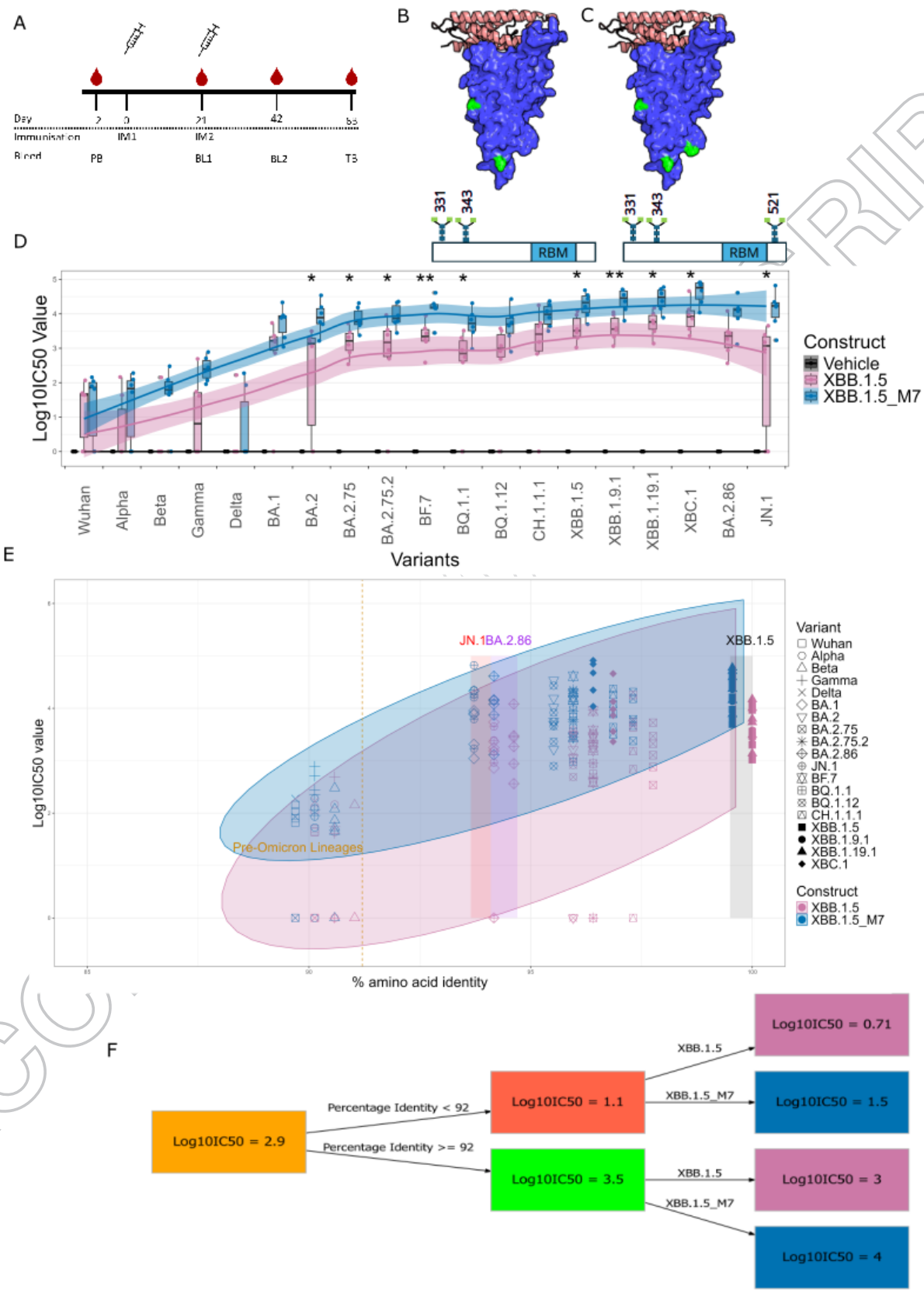
A
Day
Immunisation
Blood
PB
IM1
IM2
BL1
BL2
T3
B
C
331
343
521
RBM
D
Log10IC50 Value
Construct
Vehicle
XBB.1.5
XBB.1.5_M7
Wuhan
Alpha
Beta
Gamma
Delta
BA.1
BA.2
BA.2.75
BA.2.75.2
BF.7
BQ.1.1
BQ.1.12
CH.1.1.1
XBB.1.5
XBB.1.9.1
XBB.1.19.1
XBC.1
BA.2.86
JN.1
Variants
E
Log10IC50 value
JN.1BA.2.86
XBB.1.5
Pre-Omicron Lineages
% amino acid identity
Variant
Wuhan
Alpha
Beta
Gamma
Delta
BA.1
BA.2
BA.2.75
BA.2.75.2
BA.2.86
JN.1
BF.7
BQ.1.1
BQ.1.12
CH.1.1.1
XBB.1.5
XBB.1.9.1
XBB.1.19.1
XBC.1
Construct
XBB.1.5
XBB.1.5_M7
F
Log10IC50 = 2.9
Percentage Identity < 92
Percentage Identity >= 92
Log10IC50 = 1.1
Log10IC50 = 3.5
XBB.1.5
XBB.1.5_M7
XBB.1.5
XBB.1.5_M7
Log10IC50 = 0.71
Log10IC50 = 1.5
Log10IC50 = 3
Log10IC50 = 4

Figure captions:

Figure 1. A: Immunisation schematic showing dates of immunisations and bleeds (PB, pre-bleed, BL1, bleed 1, BL2, bleed 2, TB, terminal bleed. IM1/IM2, immunisation 1 or 2). **B, C**: cartoon diagram of the SARS-CoV-2 XBB.1.5 RBD in complex with ACE-2 (pink). Glycosylation sites shown in green for XBB.1.5 (B) and the glycan masked construct (C). **D**: Visualisation of the $Log_{10}IC_{50}$ values obtained through pseudotype virus microneutralisation assay with guinea pig serum after two immunisations with mRNA vaccines. The constructs against the different variants is given using box-and-whisker plots. A regression line (method = LOESS) with shaded confidence interval was added. The colours for the graph indicate the three constructs: Vehicle/naïve (black), XBB.1.5/WT (pink), XBB.1.5_M7 (blue). Mann-Whitney U-tests were performed to determine significance ($p < 0.05$ indicated by a single asterisk (*)). The graph was produced using the ggplot2 package in R. **E**: A scatterplot of the $Log_{10}IC_{50}$ values and percentage identity between the variant RBDs and the different constructs is given. The different variants are indicated by distinct symbols as given by the legend. XBB.1.5/WT is given in pink, while XBB.1.5_M7 is given in blue. The different rectangles indicate the $Log_{10}IC_{50}$ values for both constructs for BA.2.86 (purple), JN.1 (red), and XBB.1.5 (black). A dashed dark yellow line indicates the separation between pre-Omicron variants and subsequent Omicron variants. The ellipse indicates the 95% confidence level. The graph was produced using the ggplot2 package in R. **F:** A regression tree indicating the $Log_{10}IC_{50}$ value for the constructs when accounting for percentage identity. The regression tree model was produced using the R package rpart, while the plot was created using rpart.plot and DiagrammeR. The rules for the regression tree are as follows:

Log_{10}IC50_Value		cover
0.71	when Percentage_Identity < 92 & Construct is XBB.1.5	13%
1.5	when Percentage_Identity < 92 & Construct is XBB.1.5_M7	13%
3	when Percentage_Identity >= 92 & Construct is XBB.1.5	37%
4	when Percentage_Identity >= 92 & Construct is XBB.1.5_M7	37%

Enhanced variant neutralisation through glycan masking of SARS-CoV-2 XBB1.5 RBD

Authors

Joey Olivier[1], Charlotte George[1], Chloe Qingzhou Huang[1], Sneha B. Sujit[2], Paul Tonks[1], Diego Cantoni[3], Joe Grove[3], Laura O'Reilly[1], Johannes Geiger[5], Christian Dohmen[5], Verena Mummert[5], Anne Rosalind Samuel[5], Christian Plank[5], Rebecca Kinsley[2], Nigel Temperton[4], Martina Pfranger[6,7], Ralf Wagner[6,7], Jonathan L Heeney[1,2], Sneha Vishwanath[1,2*], George W. Carnell[1,2,8*].

* Authors contributed equally

Cambridge

1. Lab of Viral Zoonotics, Department of Veterinary Medicine, University of Cambridge, Cambridge, UK

2. DIOSynVax Ltd, University of Cambridge, Cambridge, UK

3. MRC-University of Glasgow Centre for Virus Research, University of Glasgow, Scotland, UK

4. Viral Pseudotype Unit, Medway School of Pharmacy, The Universities of Kent and Greenwich at Medway, Chatham, UK

5. Ethris GmbH, Planegg, Germany

6. Institute of Medical Microbiology and Hygiene, University of Regensburg, Regensburg, Germany

7. Institute of Clinical Microbiology and Hygiene, University Hospital Regensburg, Regensburg, Germany

8. One Virology, Wolfson Centre for Global Virus Research, School of Veterinary Medicine and Science, University of Nottingham, United Kingdom

Supplementary Materials

Materials and Methods

Design of vaccine constructs

The sequence of the SARS-CoV-2 XBB.1.5 RBD was constructed as a consensus from XBB.1.5 strains obtained from NCBI genbank, and a glycosylation site was introduced at the CR3022 monoclonal antibody binding site to produce XBB1.5_M7. In-silico mutation of animo acids in the sequon N-X-T was carried out using the FoldX algorithm[1,2]. Briefly, two positions - 381 and 521 were chosen to introduce the glycosylation site in the XBB.1.5 RBD. The structure of the RBD was extracted from PDB id - 8V0R and first repaired using the Repair module of the FOLDx algorithm. The energy of the mutants was calculated using the BuildRepair module of FOLDx algorithm. Total 5 runs were performed for the BuildRepair module. We calculated the mutations with the least energy cost and used these in the design of XBB1.5_M7. Data shown in Supplementary Table 1

Cells

HEK293T/17 (ATCC: CRL-11268) cells were maintained and grown in Dulbecco's MEM (DMEM) supplemented with 10% Fetal Bovine Serum (FBS, Merck) and 1% Penicillin/Streptomycin (Pen/Strep, Thermo Fisher) at 37°C and 5% CO2 in a humidified incubator.

Pseudotype virus production

Lentiviral pseudotypes were produced by transient transfection of HEK293T/17 cells with packaging plasmids p8.91[3,4] and pCSFLW[5] and different SARS-CoV-2 VOC spike-bearing expression plasmids using the Fugene-HD (Promega) transfection reagent[6,7]. 6-well plates pre-seeded with $2x10^5$ HEK293T/17 cells were transfected with 250 ng of p8.91, 375 ng of pCSFLW and 10-100 ng of pEVAC or pCAGGS spike bearing plasmids in 100 µl Opti-MEM for each well of a 6-well plate for transfection. Fugene-HD was added at 3 µl to 1 µg DNA ratio and incubated with DNA mixes for 15 minutes at R.T. Supernatants were harvested after 48h, passed through a 0.45 µm cellulose acetate filter (Merck Millipore), and titrated on HEK293T/17 cells transiently expressing human ACE-2 and TMPRSS2. Target HEK293T/17 cells were transfected 24h prior in a T75 flask with 2 µg pCAGGS-huACE-2 and 150 ng pCAGGS-TMPRSS2[8,9].

Flow cytometry binding analysis of vaccine antigen expression

Naked vaccine mRNAs were transfected into HEK293T/17 cells using Lipoectamine MessengerMax transfection reagent (Thermo Fisher Scientific, cat LMRNA001). This assay was performed in triplicate or quadruplicate using 96-well plates 24h after 30,000 cells were seeded per well. 100 ng of mRNA was transfected per well with a 1:10 ratio of MessengerMax to Opti-MEM and incubated at R.T for 10 minutes. 24h after transfection, cells were detached with 0.25% Trypsin-EDTA and seeded into a 96-well V-bottom dilution plate for antibody staining. Briefly, cells were centrifuged at 300 x *g* for 2 minutes to pellet them, and washed with PBS -/-, 1% FBS. This was carried out twice, and cells resuspended in 50 µl PBS -/-, 1% FBS containing 2 µg/ml of CR3022 or S309, or 1:200 NIBSC serum

21/338 (https://nibsc.org/documents/ifu/21-338.pdf). Cells were incubated for 30 minutes at R.T, washed twice as previously and then incubated with secondary antibody (goat anti human AF647, Thermo Fisher Scientific) at 6 µg/ml in a volume of 50 µl for 30 minutes in the dark. Cells were then washed twice as previously, resuspended in 200 µl PBS -/-, 1% FBS including 7-AAD live/dead stain (Thermo Fisher, cat A1310) and read using the Attune NxT with autosampler (Thermo Fisher Scientific). Cells were gated for live singlets and then median fluorescence intensity was measured for bright far-red fluorescence. Untransfected and transfected controls for each transfected construct were tested with primary and/or secondary only controls to measure background fluorescence and used in the interpretation of the results.

Animal Work

Immunogenicity work was carried out in adult 8–10-week-old female Hartley Guinea pigs (Envigo/Inotiv). Two immunisations with a 21-day interval were performed by intramuscular injection. 100 µl of vehicle containing 15 µg lipid formulated mRNA was injected into each hind leg per immunisation. Blood was taken from the saphenous vein at day 21 and 42, three weeks after first and second immunisations. A final bleed was taken by cardiac puncture under terminal anaesthesia on day 63. Animal was carried out in accordance with U.K law through home office approved project license PP9157246. Ethics were approved by The Animal Welfare and Ethical Review Body and work carried out at University Biomedical Sciences facilities, University of Cambridge. Only data generated from the terminal serum (D63) is presented in this research letter.

Pseudotype-based microneutralisation assays

Pseudotype based microneutralisation assay was performed as described previously[10]. Briefly, serial dilutions of serum (terminal bleed only, collected on day 63, after second dose of mRNA vaccine) were incubated with SARS-CoV-2 spike bearing lentiviral pseudotypes for 1h at 37°C, 5% CO2 in 96-well white cell culture plates. 1.5x10^4 HEK293T/17 transiently expressing human ACE-2 and TMPRSS2 were then added per well and plates incubated for 48h at 37°C, 5% CO2 in a humidified incubator. Bright-Glo (Promega) was then added to each well and luminescence was read after a five-minute incubation period. Experimental data points were normalised to 100% and 0% neutralisation controls and non-linear regression analysis (Equation: log(inhibitor) vs. normalized response - Variable slope) performed to produce neutralisation curves and associated IC50 values. Internal standards consisting of a pool of sera from SARS-CoV-2 immunised animals as well as human international standards (NIBSC 21/338) were used to calibrate this assay.

Pairwise comparison

Jalview version 2.11.3.2[11] was used to perform pairwise comparisons of the RBD sequences. Consensus sequences were used for the respective RBD sequences.

Data and Statistical Analysis

Neutralisation data was analysed and Log10IC50 values were determined using GraphPad Prism version 10.2.3 for Windows, GraphPad Software, Boston, Massachusetts USA (www.graphpad.com). R Statistical Software (v4.3.3; R Core Team 2024)[12], using RStudio

(Rstudio Team, 2024), was used to create graphs and perform statistical analyses. Mann-Whitney U-tests were used to determine the significance of Log10IC50 values between constructs, and False-Discovery Rate adjustment was used for all p-values. The effects of construct choice and percentage identity between variants and constructs on Log10IC50 values were examined using regression tree models estimated using the rpart package[13].

Supplementary figures

Supplementary Table 1: Differences in the energies of the vaccine antigen XBB.1.5_M7_TM_RBD with respect to XBB.1.5_TM_RBD. A total of 5 runs were carried out for the energy calculations presented. The standard deviation (SD), the mean total energy and mean of the components energies are reported.

Position	SD	Total energy	Backbone Hbond	Sidechain Hbond	Van der Waals	Electrostatics
381	0.034509	1.17907	-0.46374	-0.46374	-0.46374	-0.75132
521	0.000905	0.673453	-0.49545	-0.49545	-0.49545	-0.01453

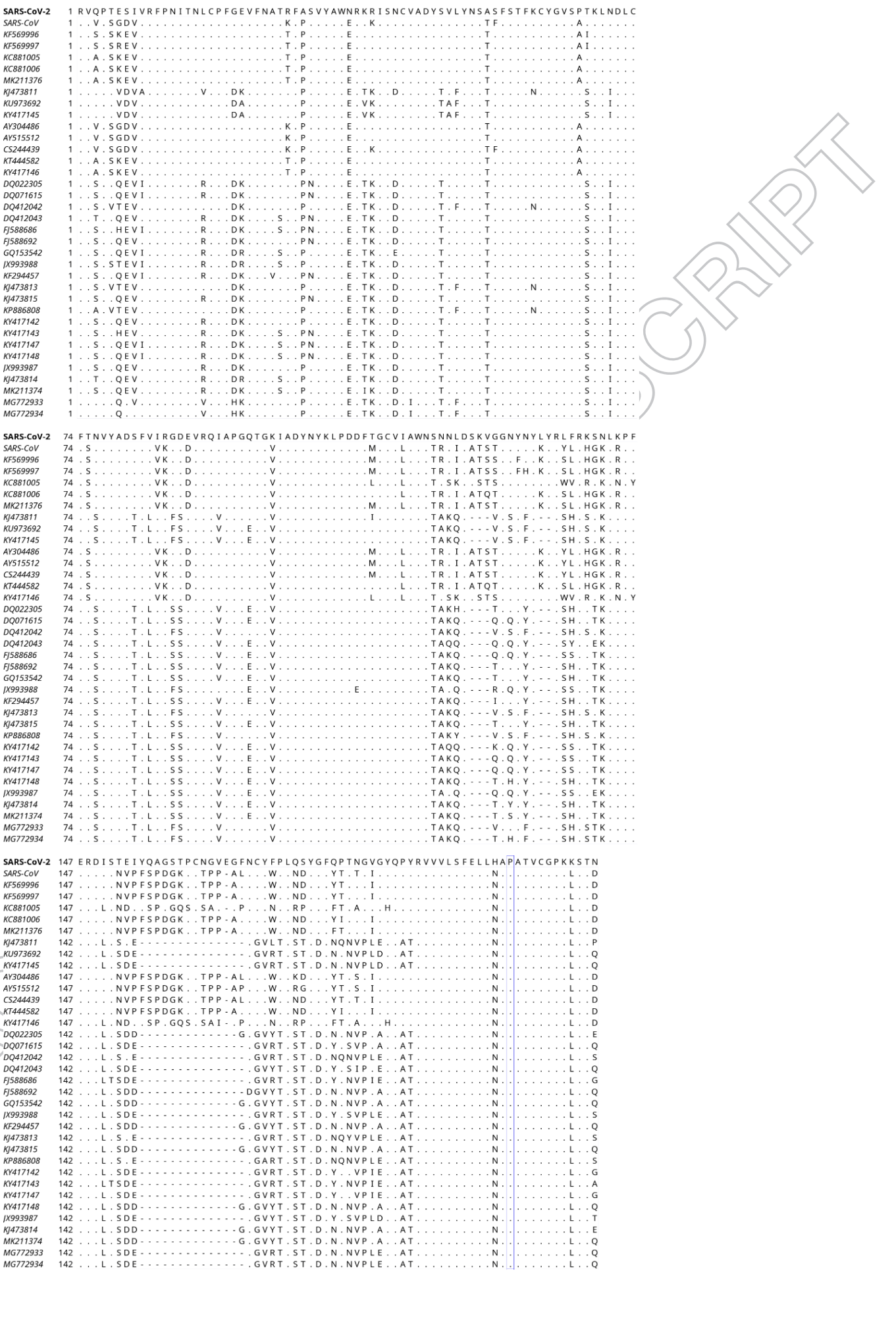
SARS-CoV-2 1 RVQPTESIVRFPNITNLCPFGEVFNATRFASVYAWNRKRISNCVADYSVLYNSASFSTFKCYGVSPTKLNDLC
SARS-CoV 1 ..V.SGDV.....K.P.....E..K.....TF.....A.....
KF569996 1 ..S.SKEV.....T.P.....E.....T.....AI.....
KF569997 1 ..S.SREV.....T.P.....E.....T.....AI.....
KC881005 1 ..A.SKEV.....T.P.....E.....T.....A.....
KC881006 1 ..A.SKEV.....T.P.....E.....T.....A.....
MK211376 1 ..A.SKEV.....T.P.....E.....T.....A.....
KJ473811 1 .....VDVA.....V...DK.....P.....E.TK..D.....T.F...T.....N.....S..I...
KU973692 1 .....VDV.....DA.....P.....E.VK.....TAF...T.....S..I...
KY417145 1 .....VDV.....DA.....P.....E.VK.....TAF...T.....S..I...
AY304486 1 ..V.SGDV.....K.P.....E.....T.....A.....
AY515512 1 ..V.SGDV.....K.P.....E.....T.....A.....
CS244439 1 ..V.SGDV.....K.P.....E..K.....TF.....A.....
KT444582 1 ..A.SKEV.....T.P.....E.....T.....A.....
KY417146 1 ..A.SKEV.....T.P.....E.....T.....A.....
DQ022305 1 ..S..QEVI.....R...DK.....PN....E.TK..D.....T.....T.....S..I...
DQ071615 1 ..S..QEVI.....R...DK.....PN....E.TK..D.....T.....T.....S..I...
DQ412042 1 ..S.VTEV.....DK.....P.....E.TK..D.....T.F...T.....N.....S..I...
DQ412043 1 ..T..QEV.....R...DK....S..PN....E.TK..D.....T.....T.....S..I...
FJ588686 1 ..S..HEVI.....R...DK....S..PN....E.TK..D.....T.....T.....S..I...
FJ588692 1 ..S..QEV.....R...DK.....PN....E.TK..D.....T.....T.....S..I...
GQ153542 1 ..S..QEVI.....R...DR....S..P.....E.TK..E.....T.....T.....S..I...
JX993988 1 ..S.STEVI.....R...DR....S..P.....E.TK..D.....T.....T.....S..I...
KF294457 1 ..S..QEVI.....R...DK...V...PN....E.TK..D.....T.....T.....S..I...
KJ473813 1 ..S.VTEV.....DK.....P.....E.TK..D.....T.F...T.....N.....S..I...
KJ473815 1 ..S..QEV.....R...DK.....PN....E.TK..D.....T.....T.....S..I...
KP886808 1 ..A.VTEV.....DK.....P.....E.TK..D.....T.F...T.....N.....S..I...
KY417142 1 ..S..QEV.....R...DK.....P.....E.TK..D.....T.....T.....S..I...
KY417143 1 ..S..HEV.....R...DK....S..PN....E.TK..D.....T.....T.....S..I...
KY417147 1 ..S..QEVI.....R...DK....S..PN....E.TK..D.....T.....T.....S..I...
KY417148 1 ..S..QEVI.....R...DK....S..PN....E.TK..D.....T.....T.....S..I...
JX993987 1 ..S..QEV.....R...DK.....P.....E.TK..D.....T.....T.....S..I...
KJ473814 1 ..T..QEV.....R...DR....S..P.....E.TK..D.....T.....T.....S..I...
MK211374 1 ..S..QEV.....R...DK....S..P.....E.IK..D.....T.....T.....S..I...
MG772933 1 .....Q.V.....V...HK.....P.....E.TK..D.I...T.F...T.....S..I...
MG772934 1 .....Q.....V...HK.....P.....E.TK..D.I...T.F...T.....S..I...
SARS-CoV-2 74 FTNVYADSFVIRGDEVRQIAPGQTGKIADYNYKLPDDFTGCVIAWNSNNLDSKVGGNYNYLYRLFRKSNLKPF
SARS-CoV 74 .S.....VK..D.....V.....M...L...TR.I.ATST.....K..YL.HGK.R..
KF569996 74 .S.....VK..D.....V.....M...L...TR.I.ATSS..F..K..SL.HGK.R..
KF569997 74 .S.....VK..D.....V.....M...L...TR.I.ATSS..FH.K..SL.HGK.R..
KC881005 74 .S.....VK..D.....V.....L...L...T.SK..STS.....WV.R.K.N.Y
KC881006 74 .S.....VK..D.....V.....L...L...TR.I.ATQT.....K..SL.HGK.R..
MK211376 74 .S.....VK..D.....V.....M...L...TR.I.ATST.....K..SL.HGK.R..
KJ473811 74 ..S...T.L..FS....V.....V.....I.....TAKQ.---V.S.F.---SH.S.K....
KU973692 74 ..S...T.L..FS....V...E..V.....TAKQ.---V.S.F.---SH.S.K....
KY417145 74 ..S...T.L..FS....V...E..V.....TAKQ.---V.S.F.---SH.S.K....
AY304486 74 .S.....VK..D.....V.....M...L...TR.I.ATST.....K..YL.HGK.R..
AY515512 74 .S.....VK..D.....V.....M...L...TR.I.ATST.....K..YL.HGK.R..
CS244439 74 .S.....VK..D.....V.....M...L...TR.I.ATST.....K..YL.HGK.R..
KT444582 74 .S.....VK..D.....V.....L...L...TR.I.ATQT.....K..SL.HGK.R..
KY417146 74 .S.....VK..D.....V.....L...L...T.SK..STS.....WV.R.K.N.Y
DQ022305 74 ..S...T.L..SS....V...E..V.....TAKH.---T...Y.---SH..TK....
DQ071615 74 ..S...T.L..SS....V...E..V.....TAKQ.---Q.Q.Y.---SH..TK....
DQ412042 74 ..S...T.L..FS....V.....V.....TAKQ.---V.S.F.---SH.S.K....
DQ412043 74 ..S...T.L..SS....V...E..V.....TAQQ.---Q.Q.Y.---SY..EK....
FJ588686 74 ..S...T.L..SS....V...E..V.....TAKQ.---Q.Q.Y.---SS..TK....
FJ588692 74 ..S...T.L..SS....V...E..V.....TAKQ.---T...Y.---SH..TK....
GQ153542 74 ..S...T.L..SS....V...E..V.....TAKQ.---T...Y.---SH..TK....
JX993988 74 ..S...T.L..FS.....E..V.....E.....TA.Q.---R.Q.Y.---SS..TK....
KF294457 74 ..S...T.L..SS....V...E..V.....TAKQ.---I...Y.---SH..TK....
KJ473813 74 ..S...T.L..FS....V.....V.....TAKQ.---V.S.F.---SH.S.K....
KJ473815 74 ..S...T.L..SS....V...E..V.....TAKQ.---T...Y.---SH..TK....
KP886808 74 ..S...T.L..FS....V.....V.....TAKY.---V.S.F.---SH.S.K....
KY417142 74 ..S...T.L..SS....V...E..V.....TAQQ.---K.Q.Y.---SS..TK....
KY417143 74 ..S...T.L..SS....V...E..V.....TAKQ.---Q.Q.Y.---SS..TK....
KY417147 74 ..S...T.L..SS....V...E..V.....TAKQ.---Q.Q.Y.---SS..TK....
KY417148 74 ..S...T.L..SS....V...E..V.....TAKQ.---T.H.Y.---SH..TK....
JX993987 74 ..S...T.L..SS....V...E..V.....TA.Q.---Q.Q.Y.---SS..EK....
KJ473814 74 ..S...T.L..SS....V...E..V.....TAKQ.---T.Y.Y.---SH..TK....
MK211374 74 ..S...T.L..SS....V...E..V.....TAKQ.---T.S.Y.---SH..TK....
MG772933 74 ..S...T.L..FS....V.....V.....TAKQ.---V...F.---SH.STK....
MG772934 74 ..S...T.L..FS....V.....V.....TAKQ.---T.H.F.---SH.STK....
SARS-CoV-2 147 ERDISTEIYQAGSTPCNGVEGFNCYFPLQSYGFQPTNGVGYQPYRVVVLSFELLHAPATVCGPKKSTN
SARS-CoV 147 .....NVPFSPDGK..TPP-AL...W..ND...YT.T.I.....N.....L..D
KF569996 147 .....NVPFSPDGK..TPP-A....W..ND...YT...I.....N.....L..D
KF569997 147 .....NVPFSPDGK..TPP-A....W..ND...YT...I.....N.....L..D
KC881005 147 ...L.ND..SP.GQS.SA..P...N..RP...FT.A...H.....N.....L..D
KC881006 147 .....NVPFSPDGK..TPP-A....W..ND...YI...I.....N.....L..D
MK211376 147 .....NVPFSPDGK..TPP-A....W..ND...FT...I.....N.....L..D
KJ473811 142 ...L.S.E----------GVLT.ST.D.NQNVPLE..AT.....N.....L..P
KU973692 142 ...L.SDE----------GVRT.ST.D.N.NVPLD..AT.....N.....L..Q
KY417145 142 ...L.SDE----------GVRT.ST.D.N.NVPLD..AT.....N.....L..Q
AY304486 147 .....NVPFSPDGK..TPP-AL...W..KD...YT.S.I.....N.....L..D
AY515512 147 .....NVPFSPDGK..TPP-AP...W..RG...YT.S.I.....N.....L..D
CS244439 147 .....NVPFSPDGK..TPP-AL...W..ND...YT.T.I.....N.....L..D
KT444582 147 .....NVPFSPDGK..TPP-A....W..ND...YI...I.....N.....L..D
KY417146 147 ...L.ND..SP.GQS.SAI-.P...N..RP...FT.A...H.....N.....L..D
DQ022305 142 ...L.SDD----------G.GVYT.ST.D.N.NVP.A..AT.....N.....L..E
DQ071615 142 ...L.SDE----------GVRT.ST.D.Y.SVP.A..AT.....N.....L..Q
DQ412042 142 ...L.S.E----------GVRT.ST.D.NQNVPLE..AT.....N.....L..S
DQ412043 142 ...L.SDE----------GVYT.ST.D.Y.SIP.E..AT.....N.....L..Q
FJ588686 142 ...LTSDE----------GVRT.ST.D.Y.NVPIE..AT.....N.....L..G
FJ588692 142 ...L.SDD----------DGVYT.ST.D.N.NVP.A..AT.....N.....L..Q
GQ153542 142 ...L.SDD----------G.GVYT.ST.D.N.NVP.A..AT.....N.....L..Q
JX993988 142 ...L.SDE----------GVRT.ST.D.Y.SVPLE..AT.....N.....L..S
KF294457 142 ...L.SDD----------G.GVYT.ST.D.N.NVP.A..AT.....N.....L..Q
KJ473813 142 ...L.S.E----------GVRT.ST.D.NQYVPLE..AT.....N.....L..S
KJ473815 142 ...L.SDD----------G.GVYT.ST.D.N.NVP.A..AT.....N.....L..Q
KP886808 142 ...L.S.E----------GART.ST.D.NQNVPLE..AT.....N.....L..S
KY417142 142 ...L.SDE----------GVRT.ST.D.Y..VPIE..AT.....N.....L..G
KY417143 142 ...LTSDE----------GVRT.ST.D.Y.NVPIE..AT.....N.....L..A
KY417147 142 ...L.SDE----------GVRT.ST.D.Y..VPIE..AT.....N.....L..G
KY417148 142 ...L.SDD----------G.GVYT.ST.D.N.NVP.A..AT.....N.....L..Q
JX993987 142 ...L.SDE----------GVYT.ST.D.Y.SVPLD..AT.....N.....L..T
KJ473814 142 ...L.SDD----------G.GVYT.ST.D.N.NVP.A..AT.....N.....L..E
MK211374 142 ...L.SDD----------G.GVYT.ST.D.N.NVP.A..AT.....N.....L..Q
MG772933 142 ...L.SDE----------GVRT.ST.D.N.NVPLE..AT.....N.....L..Q
MG772934 142 ...L.SDE----------GVRT.ST.D.N.NVPLE..AT.....N.....L..Q

Supplementary figure 1.

Multiple sequence alignment of diverse Sarbecoviruses. The Wu-Hu-1 strain (NCBI ID: NC_045512.2) is used as reference and the conserved residues are represented as dots. The position 521 which was chosen for our vaccine modification to introduce a glycan, is boxed in blue, showing conservation of the residue despite the diversity of sequences shown.

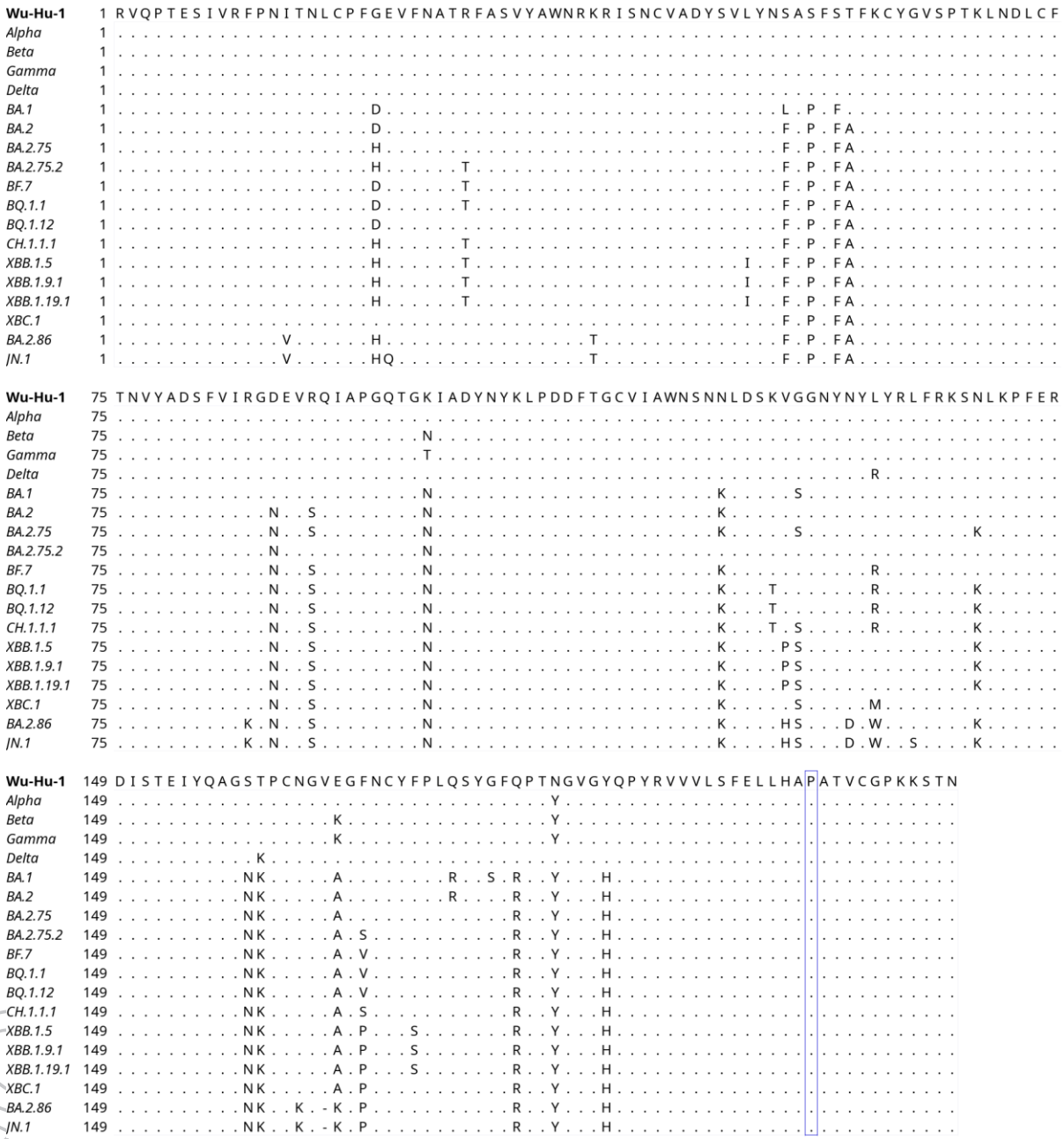

Supplementary figure 2.

Multiple sequence alignment of SARS-CoV-2 lineages. The Wu-Hu-1 strain (NCBI ID: NC_045512.2) is used as reference and the conserved residues are represented as dots.

The position 521 which was chosen for our vaccine modification to introduce a glycan, is boxed in blue, showing full conservation across the lineages from 2019 to 2024..

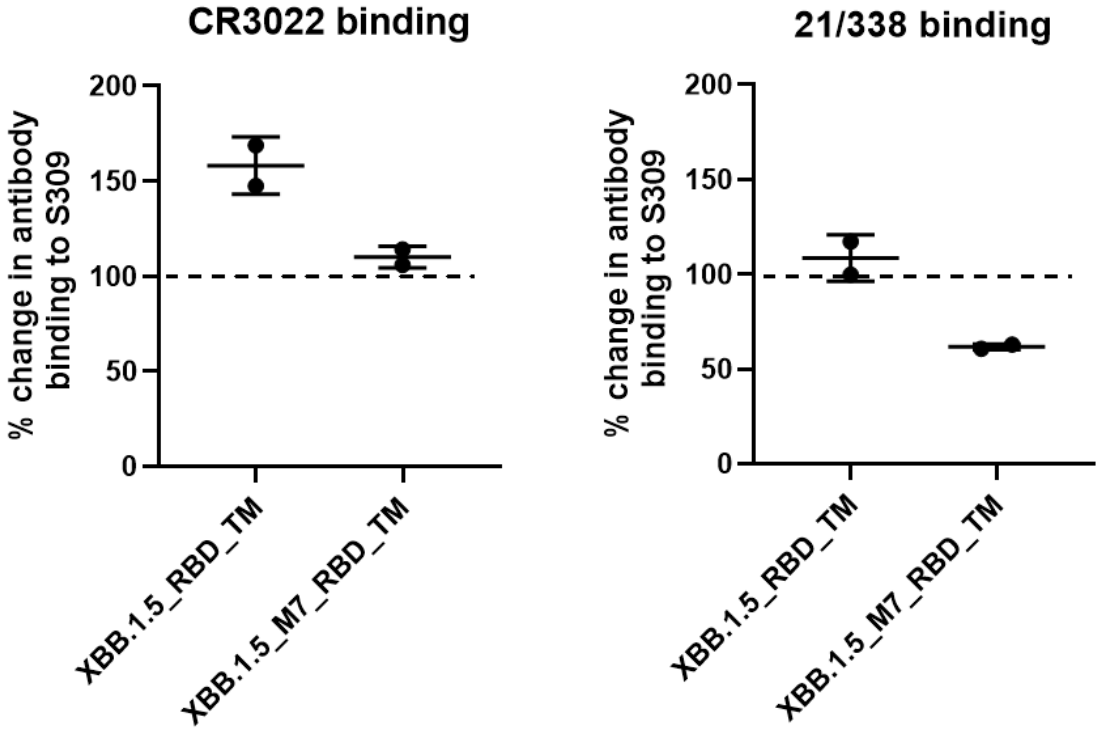

Supplementary figure 3.

Binding of antibody CR3022 and polyclonal antisera 21/338 to vaccine constructs XBB.1.5_RBD_TM and XBB.1.5_M7_RBD_TM. Values are normalised to S309 binding per construct (Geometric mean 8625 and 7940 MFI respectively) and represented by the dashed line at 100%. Binding of the antibody CR3022 is reduced for XBB.1.5_M7_RBD_TM as a result of the glycosylation site introduced to mask its binding epitope, whereas the binding of S309 is unchanged. The binding of polyclonal antisera 21/338 is also reduced for the XBB.1.5_M7_RBD_TM antigen as a result of the masked epitope.

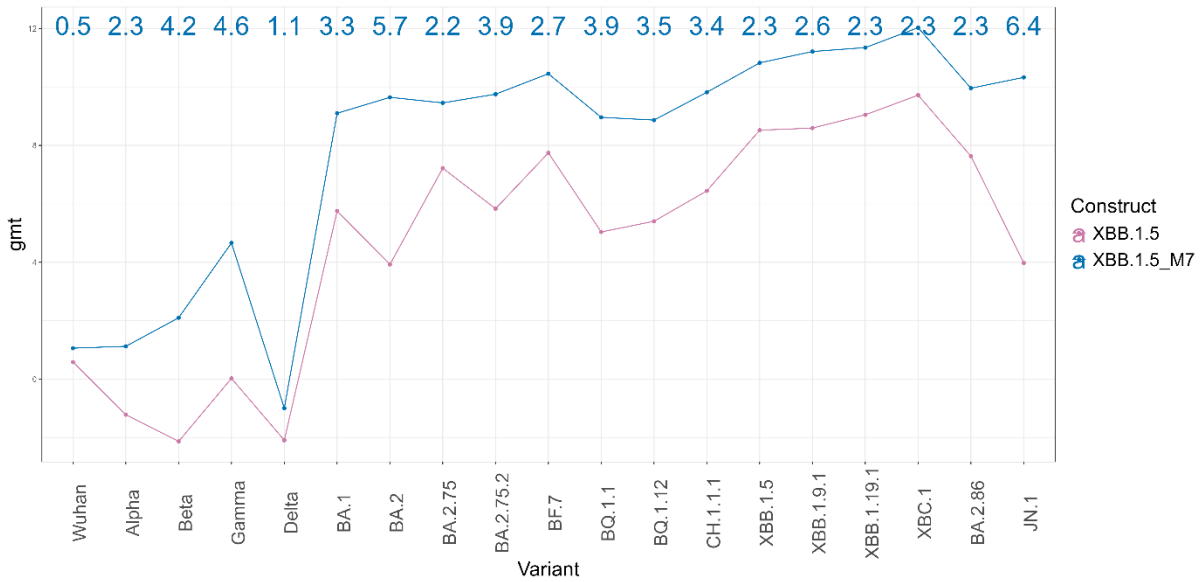

Supplementary figure 4.

Fold change in neutralising antibody titre elicited between XBB.1.5_RBD_TM and XBB.1.5_M7_RBD_TM antigens. The geometric mean titer was calculated using the titertools package[14] in RStudio on the IC50 values (blue and pink lines), returning the log2 geometric mean titer (gmt). The fold change between XBB.1.5_RBD_TM sera and XBB.1.5_M7_RBD_TM sera was calculated for each variant and is displayed by the numbers in blue, top of the graph.

References

1. Schymkowitz, J. *et al.* The FoldX web server: an online force field. *Nucleic Acids Res.* **33**, W382-388 (2005).

2. Kornfeld, R. & Kornfeld, S. Assembly of asparagine-linked oligosaccharides. *Annu. Rev. Biochem.* **54**, 631–664 (1985).

3. Zufferey, R., Nagy, D., Mandel, R. J., Naldini, L. & Trono, D. Multiply attenuated lentiviral vector achieves efficient gene delivery in vivo. *Nat. Biotechnol.* **15**, 871–875 (1997).

4. Naldini, L. *et al.* In Vivo Gene Delivery and Stable Transduction of Nondividing Cells by a Lentiviral Vector. *Science* **272**, 263–267 (1996).

5. Demaison, C. *et al.* High-Level Transduction and Gene Expression in Hematopoietic Repopulating Cells Using a Human Imunodeficiency Virus Type 1-Based Lentiviral Vector Containing an Internal Spleen Focus Forming Virus Promoter. *Hum. Gene Ther.* **13**, 803–813 (2002).

6. Sampson, A. T. *et al.* Coronavirus Pseudotypes for All Circulating Human Coronaviruses for Quantification of Cross-Neutralizing Antibody Responses. *Viruses* **13**, 1579 (2021).

7. Genova, C. *et al.* Production, Titration, Neutralisation, Storage and Lyophilisation of Severe Acute Respiratory Syndrome Coronavirus 2 (SARS-CoV-2) Lentiviral Pseudotypes. *BIO-Protoc.* **11**, (2021).

8. Hoffmann, M. *et al.* SARS-CoV-2 Cell Entry Depends on ACE2 and TMPRSS2 and Is Blocked by a Clinically Proven Protease Inhibitor. *Cell* **181**, 271-280.e8 (2020).

9. Bertram, S. *et al.* Influenza and SARS-Coronavirus Activating Proteases TMPRSS2 and HAT Are Expressed at Multiple Sites in Human Respiratory and Gastrointestinal Tracts. *PLoS ONE* **7**, e35876 (2012).

10. Carnell, G., Grehan, K., Ferrara, F., Molesti, E. & Temperton, N. An Optimized Method for the Production Using PEI, Titration and Neutralization of SARS-CoV Spike Luciferase Pseudotypes. *Bio-Protoc.* **7**, e2514 (2017).

11. Waterhouse, A. M., Procter, J. B., Martin, D. M. A., Clamp, M. & Barton, G. J. Jalview Version 2—a multiple sequence alignment editor and analysis workbench. *Bioinformatics* **25**, 1189–1191 (2009).

12. R Core Team. R: A Language and Environment for Statistical Computing. R Foundation for Statistical Computing (2024).

13. Terry Therneau, Beth Atkinson, Brian Ripley. rpart: Recursive Partitioning and Regression Trees. (2023).

14. Wilks SH (2023). titertools: A statistical toolkit for the analysis of censored titration data. R package version 0.0.0.9003.